J. Inst. Eng. India Ser. C (April 2019) 100(2):311–322
https://doi.org/10.1007/s40032-017-0438-y

ORIGINAL CONTRIBUTION

Frequency Response Studies using Receptance Coupling Approach in High Speed Spindles

Jakeer Hussain Shaik[1] · K. Ramakotaiah[1] · J. Srinivas[2]

Received: 10 April 2017 / Accepted: 22 December 2017 / Published online: 16 January 2018

Abstract In order to assess the stability of high speed machining, estimate the frequency response at the end of tool tip is of great importance. Evaluating dynamic response of several combinations of integrated spindle-tool holder-tool will consume a lot of time. This paper presents coupled field dynamic response at tool tip for the entire integrated spindle tool unit. The spindle unit is assumed to be relying over the front and rear bearings and investigated using the Timoshenko beam theory to arrive the receptances at different locations of the spindle-tool unit. The responses are further validated with conventional finite element model as well as with the experiments. This approach permits quick outputs without losing accuracy of solution and further these methods are utilized to analyze the various design variables on system dynamics. The results obtained through this analysis are needed to design the better spindle unit in an attempt to reduce the frequency amplitudes at the tool tip to improvise the milling stability during cutting process.

Keywords Receptances-coupling · Tool-tip frequency response · Flexible spindle housing · Finite element modelling · Experimental modal analysis

✉ K. Ramakotaiah
krk_ipe@yahoo.co.in

[1] Department of Mechanical Engineering, KKR and KSR Institute of Technology, Guntur, India

[2] Department of Mechanical Engineering, National Institute of Technology, Rourkela, India

Introduction

Present day industries concentrate on astounding machining and computerization innovation. Quality of work pieces and profitability are enhanced by ceaseless observing of machine devices and process. Fast machining utilizing vertical CNC processing keeps on being considerably utilized as a part of diversity of industrial sectors, particularly aviation, automobile, die industries and others. Vibration examination in metal cutting has paramount importance since vibrations may cause loss of surface finish of work pieces, reduces tool life, lowers the life of machine components and produce the abnormal sounds during machining. The vibration levels during machining primarily depend on the cutting force developed during machining and the tooth passing frequencies during the engagement of the cutting tool and the work piece. Also the fundamental mode of natural frequencies with damping coefficients and stiffness of the entire spindle-tool unit influences the vibration response magnitudes. In automated manufacturing systems, an accurate estimation of cutting force and chatter vibrations are especially required for recognizing the high-proficient, high-eminence and inexpensive milling process. Chatter oscillations continue to be a significant restricting aspect to enhance the metal removal rates of the machining process. To prevent the chatter phenomenon during the machining highly accurate dynamic models are needed which improves the surface quality. In order to get the dynamic response of the spindle-tool unit at the tool tip can be obtained by the modal testing. These tests have several limitations such as time taken for arranging the unit in particular direction and trial readings have to be taken. Further, these readings may not be accurate as the equipments become old and it is a costly experimental trail. Numerous studies have been carried out both analytically

and experimentally relating to the regenerative chatter phenomenon in milling. Garitaonandia, et al [1] developed the modal identification procedure for various components of machine tools such as drilling and milling machine. The various components of the models are assembled by the sub-structuring techniques and further the results from analytical methods are confirmed with experiments. Mehrpouya, et al [2] presented a novel technique for the identification of FRF in 3D Joints with the inverse receptance coupling methodology. Several experiments are carried out to validate the applicability of the present methodology. Kiran, et al [3] described a technique to compensate the accelerometer readings with the cable readings. Inverse coupling method had been implemented at various stages to obtain the dynamic response of the system. Joshi and Bolar [4] implemented the nonlinear finite element method to determine the frequency response for the aerospace alloys. Hung, et al [5] investigated the interaction of the machine spindle and the housing over the stability of the system with the finite element method. Tewari and Nitin [6] analytically arrived the frequency response for the metal cutting process with mild steel.

The sub-structural methods such as component mode synthesis (CMS) and receptance coupling sub structural analysis (RCSA) provides an efficient way to reduce the computational memory and the time taken for the simulation. Particularly, the RCSA is very efficient in handling the large members of the structure. Numerous authors like Schmitz and Duncan [7], Movahhedy and Gerami [8], Erturk, et al [9], Schmitz, et al [10], Zhongqun, et al [11] applied the RCSA technique to predict the frequency response at tool tip. Schmitz [12] predicted the torsional and bending receptances for the model. According to Jun, et al [13], Kumar and Schmitz [14] identified the spindle machine receptances by various methods. The numerical results were validated by the experimental techniques. Filiz, et al [15] Conventional RCSA approach employed the dynamics of different tool, too-holder combinations and spindle-device to recognize the dynamics at tool-tip. To this end, practical requirement of four spindle-device receptances causes the method to be sometimes inaccurate. Furthermore, Albertelli, et al [16] developed a new technique which eliminates the moment and rotational receptances of the structure and provides more accurate results. Mancisidor, et al [17] investigated a new methodology of evaluating the dynamic behaviour of the sub structures. Leonesioa, et al [18] identified the different model techniques in frequency domain for the grinding machine tool. The stiffness and damping are obtained by using the closed loop frequency response method. Tanuja and Chatterjee [19] detected the acceleration response of the beam using the moving mass method using the R-K solver. Chakraborty [20] considered the linear hysteretic damping in a single degree of freedom oscillator to derive impulse response function. Montevecchi [21] developed a novel coupling method to predict the tool tip frequency response at the tool tip using the inverse receptance coupling approach.

Using the RCSA technique to arrive the frequency response at different locations is an open research area where several boundaries can be applied to improve the accuracy of the solution. In general the spindle portion can be idealised as the fixed-free beam and the rest of the elements as the free-free beam conditions. Initially the spindle has fixed in the housing portion holding the tool-holder and tool will considerable effect on the dynamic response of the system.

Present paper deals with a coupled model of a vertical end-mill spindle tool unit using RCSA by accounting flexibility of spindle unit resting on ball-bearings within the housing. One-dimensional finite element model using Timoshenko beam elements are utilized to arrive the receptance of the spindle unit. Furthermore, these analytical spindle receptance are assembled with tool and holder receptances to arrive the consequent tool tip frequency response. The response results are validated using full-order finite element analysis and 3-D analysis of solid model of the assembly. Later the parametric effects like tool overhang, spindle bearing span and bearing preload using RCSA methodology are discussed.

Receptance Coupling Methodology

In this RCSA strategy, the whole machine tool spindle unit is considered to have three essential components: the spindle-device, tool-holder, and tool. Generally, for the spindle-device receptances or frequency response functions (FRFs) can be measured directly. Further these spindle receptances are analytically assembled with the tool and holder receptances to arrive the frequency responses at tool tip. In general, the receptances of the tool and holder are acquired by the Bishop and Johnson theory by treating these elements with the free-free boundary conditions. Later these receptances are combined with spindle receptances by the analytical relationship to evaluate the tool tip receptance. In RCSA technique there are four component receptances primarily due to bending and rotation at different interfaces and boundary conditions. These four components are

$$\text{displacement to force } u_{ij} = \frac{x_i}{f_j},$$
$$\text{displacement to couple } v_{ij} = \frac{x_i}{m_j},$$
$$\text{rotation to force } w_{ij} = \frac{\theta_i}{f_j},$$
$$\text{rotation to couple } z_{ij} = \frac{\theta_i}{m_j},$$

where i, j represents the co-ordinate locations due to force and moment applications. If these two coordinates are same it is direct receptance and they are unequal called cross receptance. The single element receptances for the structure can be written as

$$Y_{ij}(\omega) = \begin{bmatrix} \frac{x_i}{f_j} & \frac{x_i}{m_j} \\ \frac{\theta_i}{f_j} & \frac{\theta_i}{m_j} \end{bmatrix} = \begin{bmatrix} u_{ij} & v_{ij} \\ w_{ij} & z_{ij} \end{bmatrix} \quad (1)$$

where (x_i, θ_i, f_i, m_i) are the displacement, rotation, force and couple applied at the location i and (x_j, θ_j, f_j, m_j) are the components applied at the location j. In order to obtain the direct an cross receptances for the tool (I) and holder (II) the coordinate locations are shown in Fig. 1.

To arrive the component receptances for the beam element-I the following equations are applied

$$Y_{11} = \begin{bmatrix} \frac{x_1}{f_1} & \frac{x_1}{m_1} \\ \frac{\theta_1}{f_1} & \frac{\theta_1}{m_1} \end{bmatrix} = \begin{bmatrix} u_{11} & v_{11} \\ w_{11} & z_{11} \end{bmatrix} \quad (2)$$

$$Y_{2a2a} = \begin{bmatrix} \frac{x_{2a}}{f_{2a}} & \frac{x_{2a}}{m_{2a}} \\ \frac{\theta_{2a}}{f_{2a}} & \frac{\theta_{2a}}{m_{2a}} \end{bmatrix} = \begin{bmatrix} u_{2a2a} & v_{2a2a} \\ w_{2a2a} & z_{2a2a} \end{bmatrix} \quad (3)$$

$$Y_{2b2b} = \begin{bmatrix} \frac{x_{2b}}{f_{2b}} & \frac{x_{2b}}{m_{2b}} \\ \frac{\theta_{2b}}{f_{2b}} & \frac{\theta_{2b}}{m_{2b}} \end{bmatrix} = \begin{bmatrix} u_{2b2b} & v_{2b2b} \\ w_{2b2b} & z_{2b2b} \end{bmatrix} \quad (4)$$

$$Y_{3a3a} = \begin{bmatrix} \frac{x_{3a}}{f_{3a}} & \frac{x_{3a}}{m_{3a}} \\ \frac{\theta_{3a}}{f_{3a}} & \frac{\theta_{3a}}{m_{3a}} \end{bmatrix} = \begin{bmatrix} u_{3a3a} & v_{3a3a} \\ w_{3a3a} & z_{3a3a} \end{bmatrix} \quad (5)$$

$$Y_{12a} = \begin{bmatrix} \frac{x_1}{f_{2a}} & \frac{x_1}{m_{2a}} \\ \frac{\theta_1}{f_{2a}} & \frac{\theta_1}{m_{2a}} \end{bmatrix} = \begin{bmatrix} u_{12a} & v_{12a} \\ w_{12a} & z_{12a} \end{bmatrix} \quad (6)$$

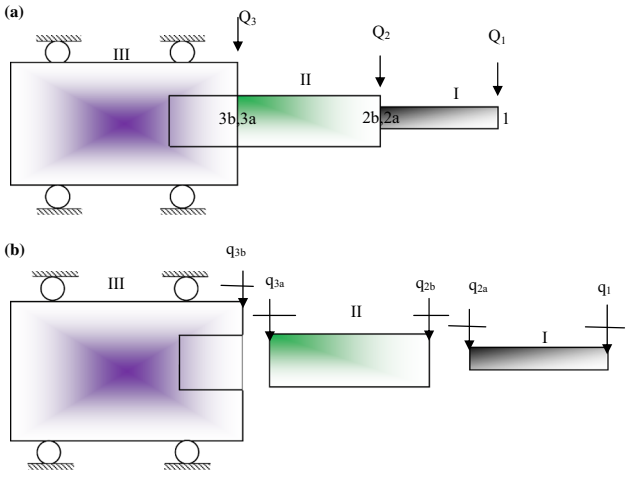

Fig. 1 Three component receptance coupling model **a** component assembly **b** individual components

$$Y_{2a1} = \begin{bmatrix} \frac{x_{2a}}{f_1} & \frac{x_{2a}}{m_1} \\ \frac{\theta_{2a}}{f_1} & \frac{\theta_{2a}}{m_1} \end{bmatrix} = \begin{bmatrix} u_{2a1} & v_{2a1} \\ w_{2a1} & z_{2a1} \end{bmatrix} \quad (7)$$

$$Y_{2b3a} = \begin{bmatrix} \frac{x_{2b}}{f_{3a}} & \frac{x_{2b}}{m_{3a}} \\ \frac{\theta_{2b}}{f_{3a}} & \frac{\theta_{2b}}{m_{3a}} \end{bmatrix} = \begin{bmatrix} u_{2b3a} & v_{2b3a} \\ w_{2b3a} & z_{2b3a} \end{bmatrix} \quad (8)$$

$$Y_{3a2b} = \begin{bmatrix} \frac{x_{3a}}{f_{2b}} & \frac{x_{3a}}{m_{2b}} \\ \frac{\theta_{3a}}{f_{2b}} & \frac{\theta_{3a}}{m_{2b}} \end{bmatrix} = \begin{bmatrix} u_{3a2b} & v_{3a2b} \\ w_{3a2b} & z_{3a2b} \end{bmatrix} \quad (9)$$

To evaluate the sub component receptances, T_{11} and T_{3a1} a force component and couple are applied at the location-1. The equations related to the displacement and the corresponding boundary conditions are applied to get sub assemble receptances for elements (I) and (II).

$$T_{11} = Y_{11} - Y_{12a}(Y_{2b2b} + Y_{2a2a})^{-1}Y_{2a1} = \begin{bmatrix} U_{11} & V_{11} \\ W_{11} & Z_{11} \end{bmatrix} \quad (10)$$

Furthermore the receptances for the coordinates 3a and 1 are as follows

$$T_{3a1} = Y_{3a2b}(Y_{3a2b} + Y_{3a2b})^{-1}Y_{2a1} = \begin{bmatrix} U_{3a1} & V_{3a1} \\ W_{3a1} & Z_{3a1} \end{bmatrix} \quad (11)$$

An equivalent force Q_{3a} is applied at the spindle location as shown in the Fig. 1a. Using this equivalent force a relationship is formed between the direct (T_{3a3a}) and cross receptances (T_{13a}) is as follows

$$T_{3a3a} = Y_{3a3a} - Y_{3a2b}(Y_{2b2b} + Y_{2a2a})^{-1}Y_{2b3a} = \begin{bmatrix} U_{3a3a} & V_{3a3a} \\ W_{3a3a} & Z_{3a3a} \end{bmatrix} \quad (12)$$

$$T_{13a} = Y_{12a}(Y_{2b2b} + Y_{2a2a})^{-1}Y_{2b3a} = \begin{bmatrix} U_{13a} & V_{13a} \\ W_{13a} & Z_{13a} \end{bmatrix} \quad (13)$$

The free component receptances of tool (I) and holder (II) with the free-free boundary conditions are coupled to the spindle (III) of the machine tool. The coupled equation of the integrated spindle-tool unit can be finally written as:

$$T'_{11} = T_{11} - T_{13a}(T_{3a3a} + Y_{3b3b})^{-1}T_{3a1} = \begin{bmatrix} U_{11} & V_{11} \\ W_{11} & Z_{11} \end{bmatrix} \quad (14)$$

In the above equation, the unknown parameter is the spindle receptance (Y_{3b3b}) and all the receptances are known. This spindle receptance can be obtained using the experimental approaches and also complicated due to the cost, cutting speeds, interface coupling etc. In the present work, this spindle receptance is easily obtained by the Finite coupling method and then coupled to the other receptances.

Spindle Receptances

The finite element method provides the more convergence solutions with repeated accuracy for complicated structures. Using the Timoshenko beam theory with rotational and bending components provides the spindle receptances. The spindle is assumed to be supported at the front and rear bearings inside the housing the machine tool as shown in the Fig. 2.

The housing portion of the machine tool is assumed to be fixed with outer races of the bearings. Spindle portion is modelled with the rotary and shear deformation effects using the Timoshenko beam theory. Ball bearing forces with Hertzian contact theory are considered to obtain the nodal displacements. In the present model, two translational moments and two rotary moments are considered at each node. The axial preload of 1500 N is considered at each bearing node position with all the other movements of the assembly. Position of the bearings, loading etc. of the angular contact ball bearings defines the stiffness behaviour of the assembly. An empirical formulae is developed in the literature with the parameters like ball diameter (D), number of rolling balls (N), contact angle between the balls (θ), axial preload (F) is considered for the analysis.

$$k_{xx} = k_{yy} = 1.77236 \times 10^7 \times \left(N^2\ D\right)^{1/3} \frac{\cos^2\theta}{\sin^{1/3}\theta} F^{1/3}\ \text{N/m} \quad (15)$$

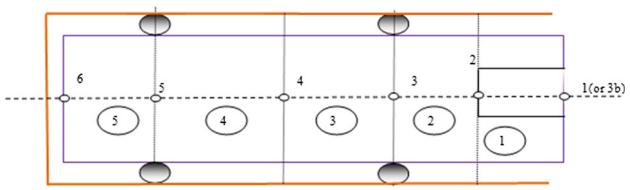

Fig. 2 Finite element model of spindle supported by housing

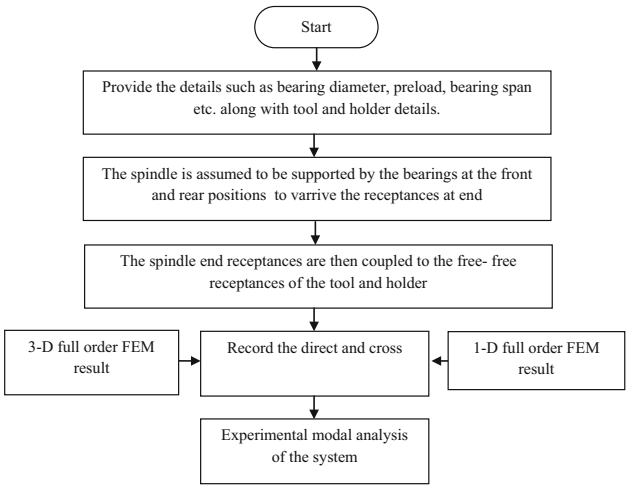

Fig. 3 The flow diagram of the approach

The assembled matrices for the mass (M_a), stiffness (K_a) and gyroscopic (G_a) are employed with consideration of above stiffness at bearings for the modelling of the spindle. The FRF made up of both real and imaginary parts as given by the Eq. (16)

Table 1 Geometric and material data of spindle-tool unit

Component	Outer lengths, mm	Outer diameter, mm	Inner diameter, mm	Young's modulus E, Pa
Tool	60	12	0	2.8×10^{11}
Holder	80	40	12	2.1×10^{11}
Spindle	248	75	40	2.1×10^{11}

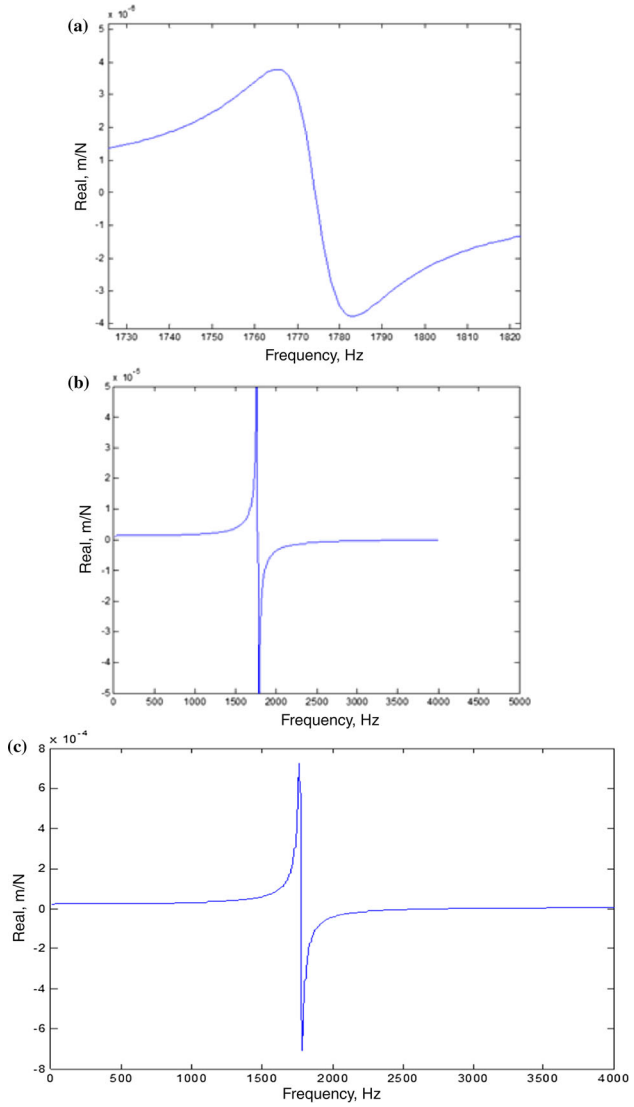

Fig. 4 Receptance T_{11} of the tool-holder sub assembly **a** real part of U_{11} **b** real part of V_{11} and W_{11} **c** real part of Z_{11}

$$[H_a(j\omega)] = [Re_a(\omega)] + j[Im_a(\omega)] = [-[M_a]\omega^2 + j\omega[[C_a] - \Omega[G_a]] + ([K_a] - \Omega^2[M_c])]^{-1} \quad (16)$$

The real (Re_a) and imaginary (Im_a) parts of the frequency response for the spindle portion are obtained by the following expressions.

$$[Re_a(G(j\omega)] = \frac{[K_a] - [M_a]\omega^2}{\sqrt{([K_a] - [M_a]\omega^2) + ([C_a]\omega)^2}} \quad (17)$$

$$[Im_a(G(j\omega)] = \frac{-[C_a]\omega}{\sqrt{([K_a] - [M_a]\omega^2) + ([C_a]\omega)^2}} \quad (18)$$

In general, the even part of the response provides the real part of the response whereas the odd part provides the imaginary part. The flow chart shown in Fig. 3 shows the overall process considered in the present work.

Results and Discussion

The geometric as well as the material properties of the integrated spindle-tool unit are taken from the workshop manuals of the MTAB- MAXMILL vertical end milling machine tool. Table 1 shows the data considered for the theoretical analysis. In the present model, 20 mm length is inserted in the tool holder, similarly 30 mm inside the spindle nose portion.

Material damping is conveniently applied to model the continuous beams with solid damping factor. The elastic

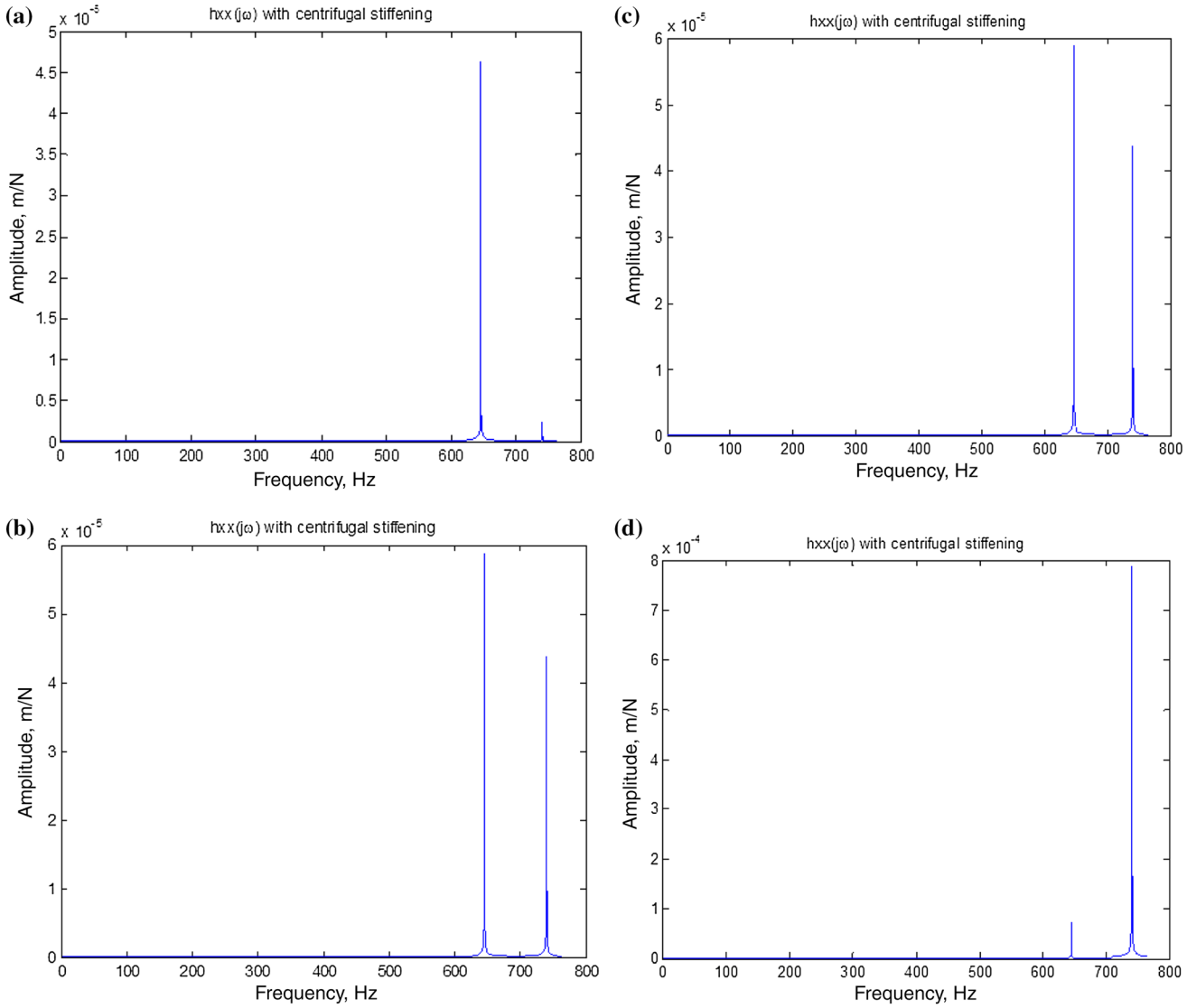

Fig. 5 Spindle machine receptances (Y_{3b3b}) obtained from finite element analysis **a** displacement to force (U_{3b3b}) **b** displacement to couple (V_{3b3b}) **c** rotation to force (W_{3b3b}) **d** rotation to couple (Z_{3b3b})

modulus is taken as $Es = E(1 + i\eta)$ where η is the solid damping factor and E is the young's modulus of elasticity. The free-free direct and cross components of receptances for the portions of the tool (I) and holder (II) are obtained by the equations as follows:

$$u_{ii} = \frac{-k_1}{\alpha^3 k_7};\ v_{ii} = \frac{k_2}{\alpha^2 k_7};\ w_{ii} = v_{ii};\ z_{ii} = \frac{k_5}{\alpha k_7} \tag{19}$$

$$u_{ij} = \frac{k_3}{\alpha^3 k_7};\ v_{ij} = \frac{-k_4}{\alpha^2 k_7};\ w_{ij} = \frac{k_4}{\alpha^2 k_7};\ z_{ij} = \frac{k_6}{\alpha k_7} \tag{20}$$

where

$$\alpha^4 = \omega^2 \frac{\rho A_s}{EI(1 + i\eta)} \tag{21}$$

$$k_1 = \cos(\alpha 1)\sinh(\alpha 1) - \sin(\alpha 1)\cosh(\alpha 1) \tag{22}$$

$$k_2 = \sin(\alpha 1)\sinh(\alpha 1) \tag{23}$$

$$k_3 = \sin(\alpha 1) - \sinh(\alpha 1) \tag{24}$$

$$k_4 = \cos(\alpha 1) - \cosh(\alpha 1) \tag{25}$$

$$k_5 = \cos(\alpha 1)\sinh(\alpha 1) + \sin(\alpha 1)\cosh(\alpha 1) \tag{26}$$

$$k_6 = \sin(\alpha 1) + \sinh(\alpha 1) \tag{27}$$

$$k_7 = E_s I(\cos(\alpha 1)\cosh(\alpha 1) - 1) \tag{28}$$

$$k_8 = E_s I(\cos(\alpha 1)\cosh(\alpha 1) + 1) \tag{29}$$

where 'l' is the length of the portion; 'ρ' is the density; 'A_s' is the cross section area of the beam. Here, ω is frequency in rad/s; A_s is beam cross-section; ρ is the density; and l is the component length. Figure 4 shows the predicted receptance T_{11} for the sub-assembly of tool and holder portions. It is observed that a frequency range of 1500 to 2000 Hz is obtained for this assembly.

For, the spindle supported on ball bearings (N = 20, D = 9 mm, F = 1500 N, and θ = 25°) within the housing, the component receptances at joint node are attained by using the finite element method as shown in Fig. 5. A frequency range of 650 to 750 Hz is observed at the spindle end consists of two bending nodes.

The spindle end receptances were further coupled to the sub-component assembled unit of the tool and holder. A program is developed in MATLAB by considering all individual receptances and coupling so as to obtain the tool-tip frequency response. Assembly receptances T_{11}' at the tool tip node are obtained as shown in Fig. 6, which is a displacement to force receptance $U_{11} = G(j\omega)$. The first bending mode at 1925 Hz is observed for the integrated spindle-tool unit at tool tip.

Figure 7 represents the picture showing the program coded for the receptance coupling approach with the appropriate boundary conditions.

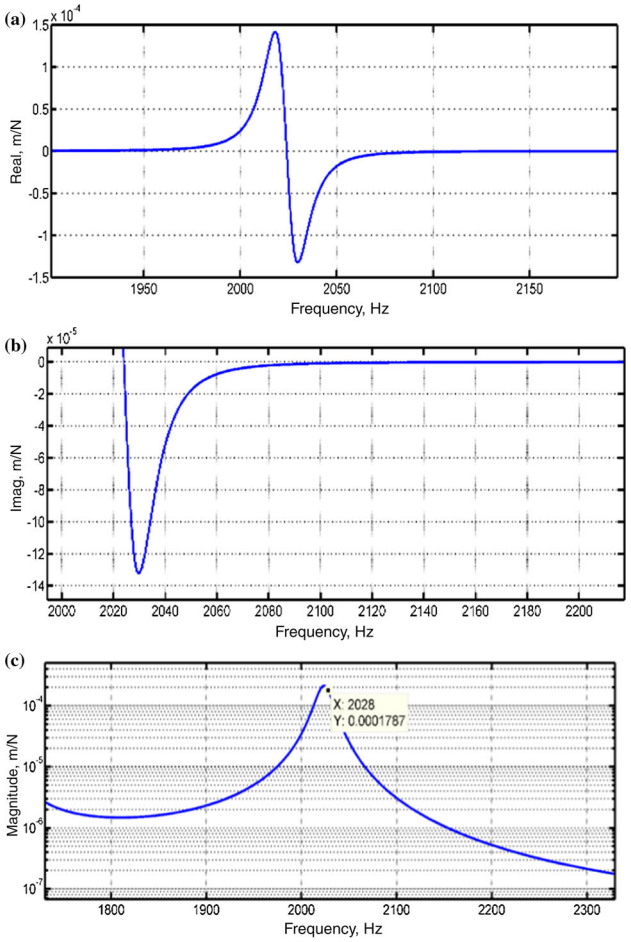

Fig. 6 Tool tip frequency response of the assembly **a** real part of U_{11} **b** Imaginary part of U_{11} **c** semi-log magnitude plot

One Dimensional Finite Element Modelling

In order to confirm the outcomes, full-order 1D finite element model is employed. As the spindle-device, tool and tool-holder assembly is relatively simple in terms of geometrical features, a combined finite element modelling of the structure with overhanging tool and tool-holder system is considered. Two-node Timoshenko beam elements are employed to discretize both spindle and tool-holder assembly. Translational and rotational inertia terms along with gyroscopic effects of each element are considered in obtaining the overall equations in matrix form as follows.

$$[M_0]\{\ddot{q}\} + [[C_o] - \Omega[G]]\{\dot{q}\} + \left([K_0] - \Omega^2[M_c]\right)\{q\} = \{F\} \tag{30}$$

The earlier equation shows various assembled terms such as the mass $[M_0]$, viscous damping $[C_0]$, stiffness $[K_0]$, gyroscopic matrices [G]. The spindle portion is supported over the same front and rear bearings as shown in the Fig. 8.

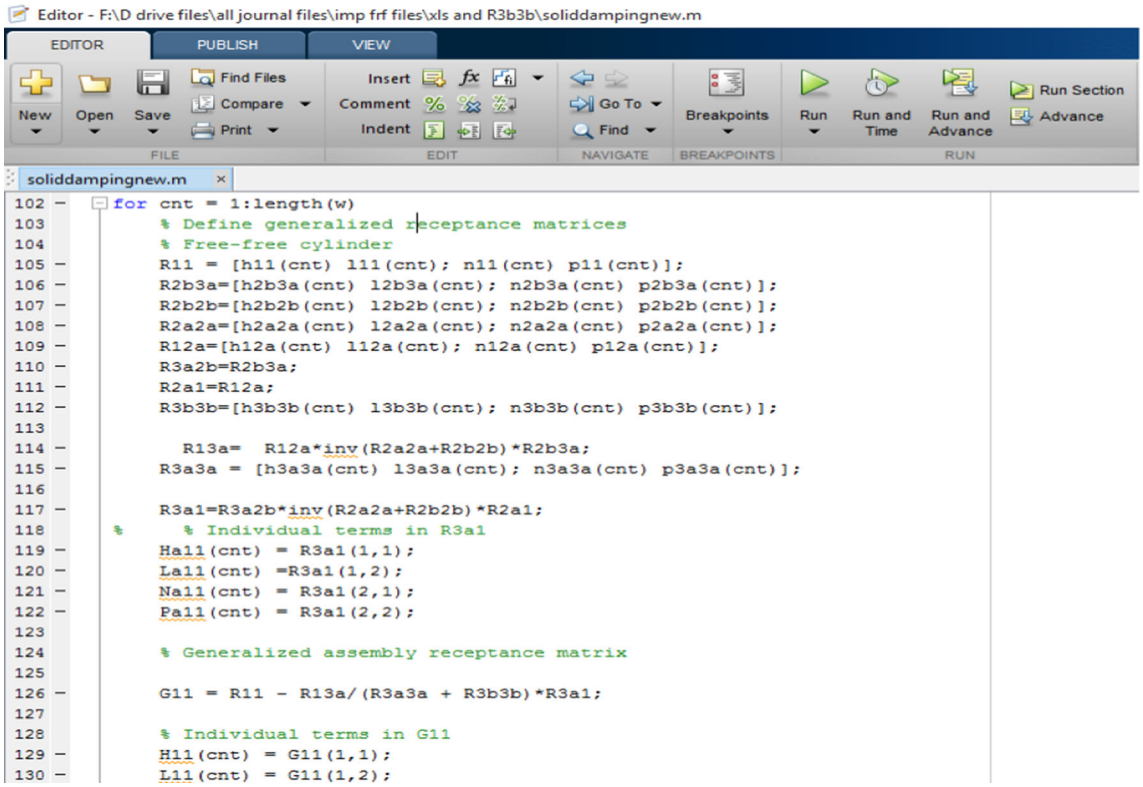

Fig. 7 MATLAB picture for tool tip frequency response of the assembly

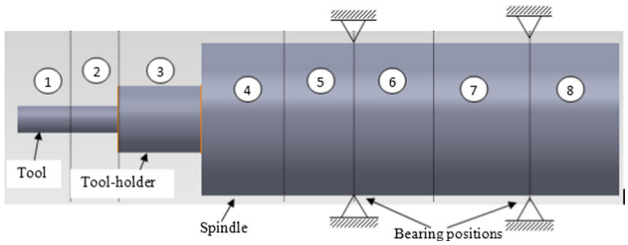

Fig. 8 Equivalent model for the finite element analysis

In general, the right choice of selecting the particular spindle-tool combination or mill head plays a key role in dynamic stability during the machining process. These high speed machine tools with higher rigidity in the integrated spindle tool portions are best suitable for machining materials like Aluminium, laminated composites, several hard alloys etc. In the present work, the M TAB mill CNC vertical milling machine has been utilized for the experiments. The machine tool has the following specifications given in Table 2.

Table 3 shows the element parameters considered for the assembly. The outer lengths and inside lengths the tool and tool-holder are taken same as the receptance coupling methodology.

Table 2 Specifications of the CNC mill spindle unit

Specifications	Units
Table travel in X, Y and Z directions	480 × 360 × 500 mm
Spindle nose taper	BT 40
Programmable spindle speed	0–10,000 rpm
Spindle motor capacity	5.5 kW
Programmable feed rate in x, y and z axis	0–6000 m/min
Max tool diameter capacity	80 mm
Maximum weight	3000 kg

Figure 9a represents the FRF for the spindle mounted on bearings. The peak frequency response is observed to be at 1959 Hz.

Three Dimensional Analysis

To confirm the first mode frequency obtained from the beam theory a similar model is considered with all the practical dimensions in 3D ANSYS workbench. The spindle-tool unit is modelled with all the geometrical dimensions and material properties in Solid Works software (Fig. 10).

Table 3 Parameters of the full-order finite element model

Parameters	Elements of the spindle tool unit							
	#1	#2	#3	#4	#5	#6	#7	#8
Length, mm	30	30	80	51	60	45	45	47
Outer diameter, mm	12	12	40	75	75	75	75	75
Inner diameter, mm	0	0	0	40	0	0	0	0
E, Pa	2.8e11	2.1e11	2.1e11	2.1e11	2.1e11	2.1e11	2.1e11	2.1e11

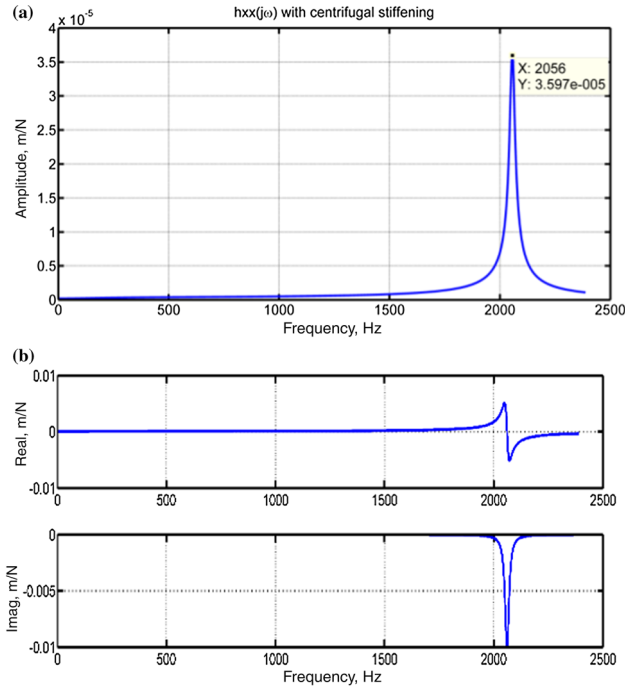

Fig. 9 Tool tip frequency responses using the full-order FEM **a** absolute FRF **b** real and imaginary FRF

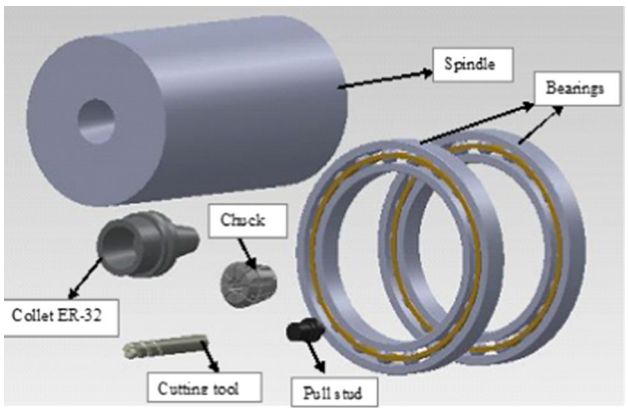

Fig. 10 Individual solid work components of MTAB MAXMILL realistic spindle system

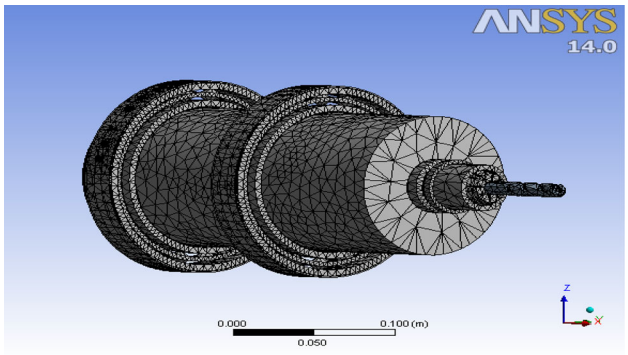

Fig. 11 Meshed model of spindle-bearing system

The IGES model of the spindle-tool unit is imported in the ANSYS workbench simulation software. Entire model is meshed with eight noded solid 187 element with the same material properties similar to the one dimensional finite element. The outer races of the two bearings are with the fixed boundary conditions whereas the inner races of the bearings are with free condition to rotate with the outer diameter of the spindle as shown in Fig. 11.

Modal analysis has been conducted to evaluate the fundamental modes of vibration. It is observed that there are first few frequencies as 2047.3, 2054.6, 2665.4, 2685.7, 2762.9, and 4481.6 kHz and their corresponding mode shapes are shown in Fig. 12. The first five modes have high deformation rates at the tool-tip and for the sixth mode the deformation is at the spindle region.

Further to validate the frequencies obtained from the modal analysis, harmonic response is carried out for the model. A sample load of 1 kN is applied at the tool tip region to arrive the frequencies to test the strength of the model. It is observed that a highest peak was obtained at a frequency of 2000 Hz which confirms the validation of the model as shown in Fig. 13.

Using the results obtained from the three modelling methods a comparative chart has been drawn showing the differences of the results as shown in Fig. 14. It is observed that the RCSA approach have a closer approximation because of considering the Timoshenko and Euler beam theories.

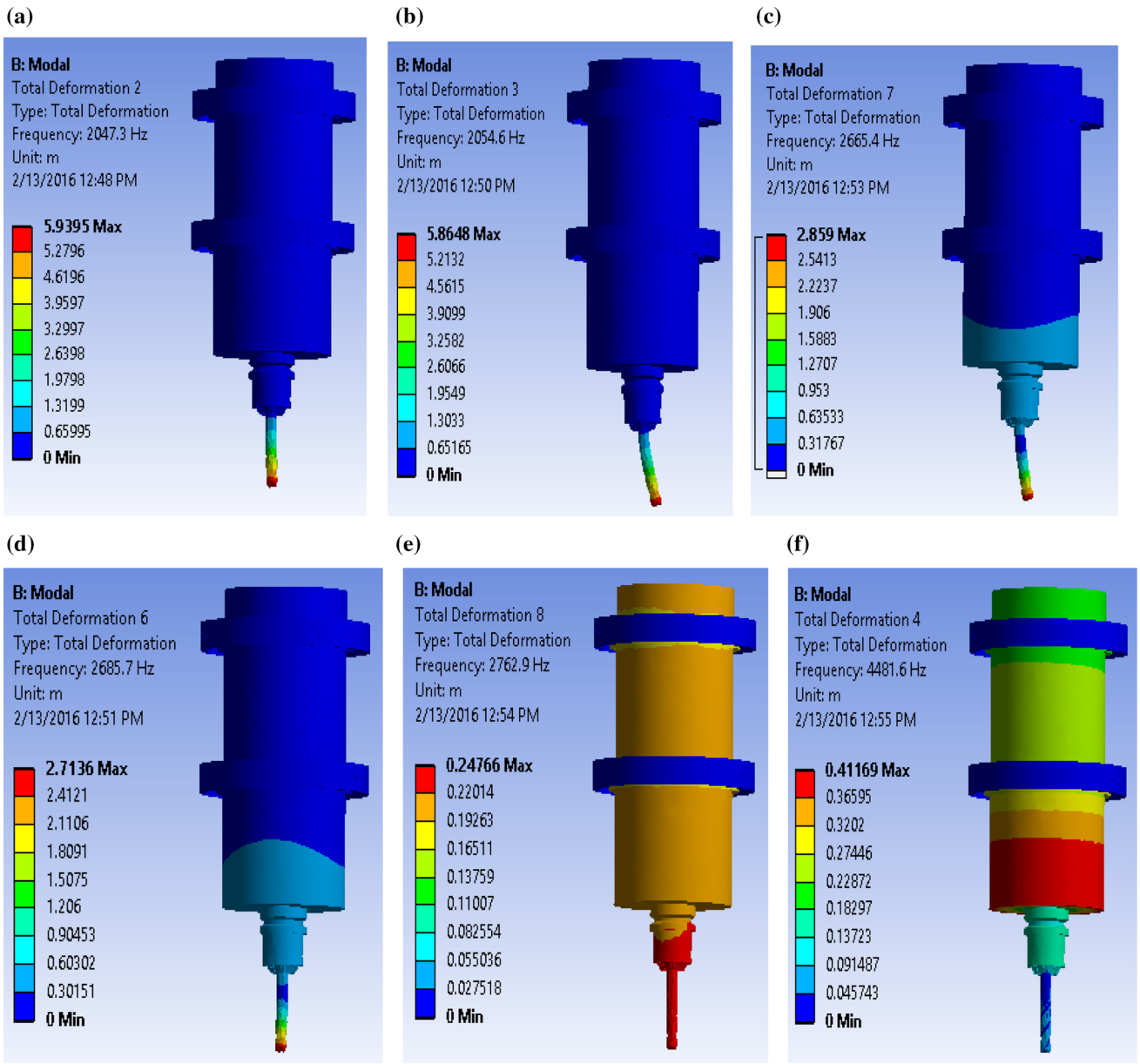

Fig. 12 Different mode vibration characteristics of spindle tool unit: **a** First mode shape. **b** Second mode shape. **c** Third mode shape. **d** Fourth mode shape. **e** Fifth mode shape. **f** Sixth mode shape

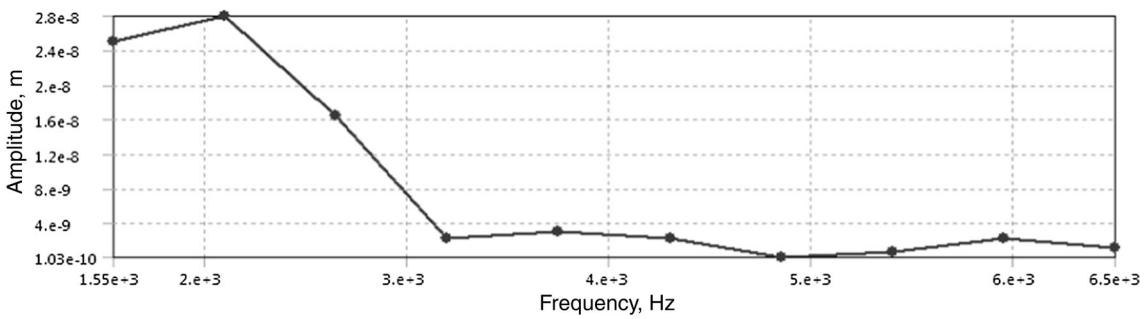

Fig. 13 Harmonic response of spindle bearing system

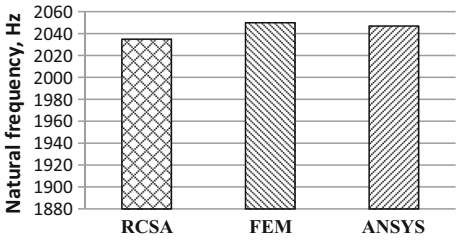

Fig. 14 Comparison of fundamental natural frequency of the system

In comparison with the 1D and 3D finite element models, the computational speed of the present approach with use of component receptances is relatively higher. On Intel Core-i7 Processor with 2 GB RAM and 1 GHz speed, the tool-tip frequency response is obtained within 20 s.

Experimental Verification using Sine Sweep Test

Further experimental studies have been conducted on the spindle-tool unit using the modal analysis to confirm the validity of the proposed approaches. A three axis vertical CNC machine MTAB made available in the NIT has been selected for the analysis. This machine tool has a AC synchronous motor with single phase available with variable speeds. Four fluted end mill cutter with 12 mm diameter is fixed in the tool holder portion. To obtain the frequencies at variable speeds the following equipments are employed: (i) an accelerometer (PG109 M0, frequency range 1 to 10,000 Hz), (ii) digital oscilloscope with four channels (model-DPO 43034), (iii) power amplifier (model SI-28), (iv) charge amplifier (model-CA 201 A0), (v) signal generator, (vi) vibration shaker (type: V-6-27050). The schematic diagrams with all the earlier equipments are shown in the Fig. 15.

The vibration shaker connected to the power amplifier excites the integrated spindle-tool unit with constant amperage of current. The frequency is varied and corresponding accelerometer readings are recorded in the oscilloscope in volts. The amplitude of the time domain signals at a frequency level are tabulated and plotted as a function of the forcing frequency as shown in Fig. 16.

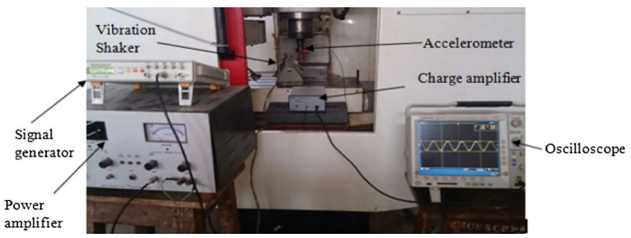

Fig. 15 Experimental set up for modal testing of the spindle tool unit

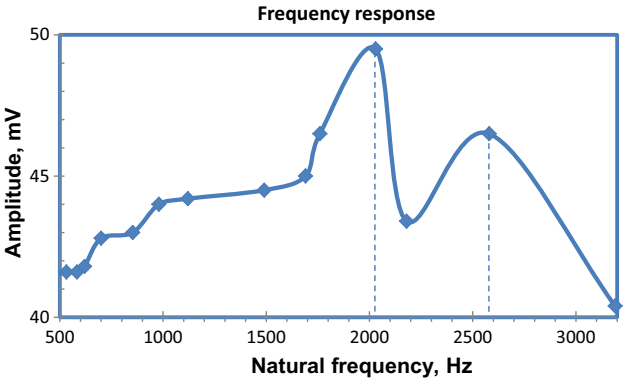

Fig. 16 Frequency response of the integral tool-spindle unit

In the sweeping range there are two peaks are observed at 2030 and 2550 Hz, respectively.

The fundamental frequency at the tool-tip obtained from receptance coupling method as 2028 Hz, finite element model as 2056.5 Hz and from the ANSYS as 2047.3 Hz are in close agreement with the experimental result.

Parametric Study of Design Parameters

In this section, the design parameters including tool overhang (TO), bearing span (BS) and bearing preload (BP)are considered in terms of their effects on the spindle modes are illustrated using RCSA methodology. Figure 17 shows the increase of tool overhanging effect of the spindle system. It has clearly observed that the first mode of frequency shifts from 1550 Hz to the left end of the response with a frequency of 716 Hz and has less effect on the dynamics of the system. The second mode responses of the two overhang lengths are mostly dominated at a frequency of 1900 Hz. This mode produces the most of the instabilities during the machining process.

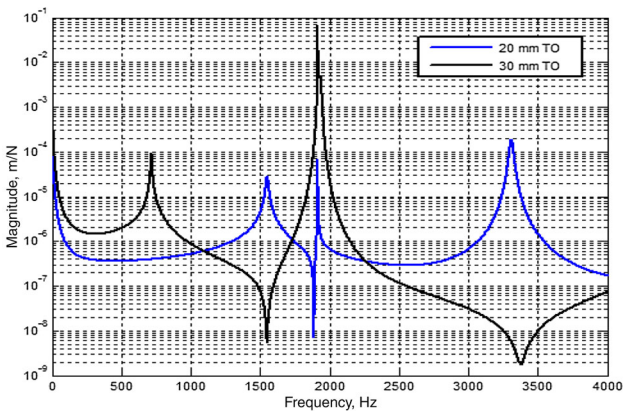

Fig. 17 Tool tip response for different lengths of tool overhang

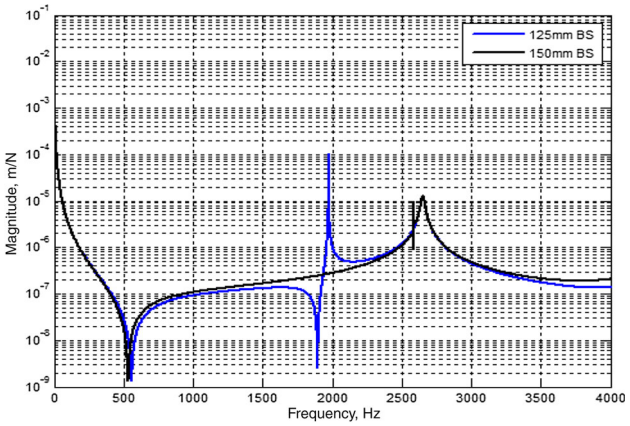

Fig. 18 Tool tip response for different lengths of bearing span ratios

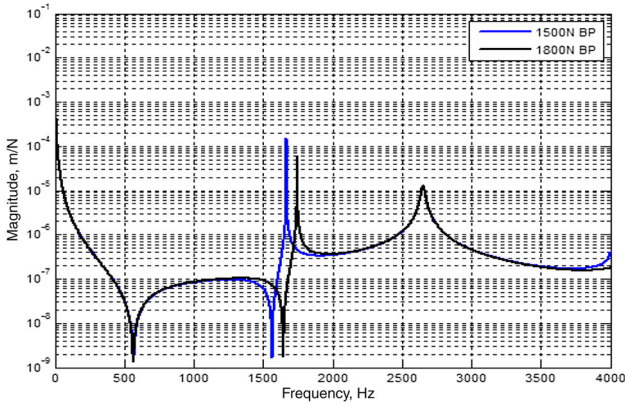

Fig. 19 Tool tip response for different values of bearing preload

Figure 18 illustrates the influence of different bearing span conditions on the spindle system are illustrated. Enhancement in the bearing span ratios the there is less distinction in the first mode and it has a natural frequency of 530 Hz. However, it is seen that second fundamental mode is altered to 1976 to 2657 Hz at the tool tip. The spindle system is little influenced by the response of the fist mode but when the span ratio is increased the vibration response of the second mode has more impact on the cutting dynamics.

Similarly, the analysis is being carried out for the bearing preload case. When the axial preload value varies from 1800 to 2000 N, it is seen that there is no clear distinction in the vibration response of first mode and the third mode. But for the second mode there is an increase in the frequency value from 1660 to 1750 Hz as shown in Fig. 19.

With the application of receptance coupling methodology, it is extremely convenient to observe the flexible dynamics at the tool tip when there are any modifications in the geometric modelling as well as in the material modelling issues of the entire spindle tool unit. From the earlier three cases, it is very keen to observe that the second mode of vibration is critically involved in changing the dynamic response at the tool tip when there is a change in the geometry of the of the spindle tool unit.

Conclusion

The present work evaluated the dynamics of an integrated spindle-tool unit of a CNC vertical machine tool with all component flexibilities. For the simulation, a practical spindle tool model with similar material and geometric data has been considered. Frequency response of the entire unit was analyzed by the modified receptance coupling approach, 1-D finite element modelling and 3D ANSYS techniques. An experimental modal analysis was also conducted in line with verification of proposed flexible spindle receptance coupling approach. It is observed that, RCSA approach has 0.08%, 1D modelling with beam theory has 1.2% and 3D ANSYS is having 0.83% deviations. In comparison with the regular practice of obtaining frequency responses experimentally, use of receptance coupling model provides a closer approximation.

Further to identify the influencing dynamic parameter on the system, the parametric studies were conducted. These techniques provides an acceptable tool-point response prediction in shortest possible time and can be effectively applied to obtain the tool tip frequency responses of the structure supported over multiple bearings. This approach finds a suitable way to handle the modular level programming to effective handle the geometric as well as the material issues at the design of more realistic spindle tool unit.

References

1. I. Garitaonandia, M.H. Fernandes, J.M. Hernandez-Vazquez, J.A. Ealo, Prediction of dynamic behavior for different configurations in a drilling–milling machine based on substructuring analysis. J. Sound Vib. **365**, 70–88 (2016)
2. M. Mehrpouya, M. Sanati, S.S. Park, Identification of joint dynamics in 3D structures through the inverse receptance coupling method. Int. J. Mech. Sci. **105**, 135–145 (2016)
3. K. Kiran, H. Satyanarayana, T. Schmitz, Compensation of frequency response function measurements by inverse RCSA. Int. J. Mach. Tools Manuf **121**, 96–100 (2017)
4. S.N. Joshi, G. Bolar, Three-Dimensional finite element based numerical simulation of machining of thin-wall components with varying wall constraints. J. Inst. Eng. (India): Ser. C. **98**(3), 343–352 (2017)
5. J.P. Hung, Y.L. Lai, T.L. Luo, H.C. Su, Analysis of the machining stability of a milling machine considering the effect of machine frame structure and spindle bearings: experimental and finite element approaches. Int. J. Adv Manuf. Technol. **68**, 2393–2405 (2013)

6. S.P. Tewari, N. Rathod, Effect of force frequency increase on depth of Cut. J. Inst. Eng (India): Ser. C. **93**(1), 47–53 (2012)
7. T.L. Schmitz, G.S. Duncan, Receptance coupling for dynamics prediction of assemblies with coincident neutral axes. J. Sound Vib. **289**, 1045–1065 (2006)
8. M.R. Movahhedy, J.M. Gerami, Prediction of spindle dynamics in milling by sub-structure coupling. Int. J. Mach. Tools Manuf. **46**, 243–251 (2006)
9. A. Erturk, H.N. Ozguven, E. Budak, Analytical modelling of spindle-tool dynamics on machine tools using Timoshenko beam model and receptance coupling for the prediction of tool point FRF. Int. J. Mach. Tools Manuf. **46**(15), 1901–1912 (2006)
10. T.L. Schmitz, K.P. Won, G.S. Duncan, W.G. Sawyer, J.C. Ziegert, Shrink fit tool holder connection stiffness/damping modelling for frequency response prediction in milling. Int. J. Mach. Tools Manuf. **47**, 1368–1380 (2007)
11. L. Zhongqun, L. Shuo, C. Yizhuang, Receptance coupling for end mill using 2-section step beam vibration model, in Second international conference on intelligent computation technology and automation. IEEE. https://doi.org/10.1109/ICICTA.2009.276 (2009)
12. T.L. Schmitz, Torsional and axial frequency response prediction by RCSA. Precis. Eng. **34**, 345–356 (2010)
13. Z. Jun, T. Schmitz, Z. Wanhua, L.U. Bingheng, Receptance coupling for tool point dynamics prediction on machine tools. Chin. J. Mech. Eng. **24**, 340–345 (2011)
14. U.V. Kumar, T.L. Schmitz, Spindle dynamics identification for receptance coupling substructure analysis. Precis. Eng. **36**, 435–443 (2012)
15. S. Filiz, C.H. Cheng, K. Powell, T. Schmitz, O. Ozdoganlar, An improved tool–holder model for RCSA tool point frequency response prediction. Precis. Eng. **33**, 26–36 (2009)
16. P. Albertelli, M. Goletti, M. Monno, A new receptance coupling substructure analysis methodology to improve chatter-free cutting conditions prediction. Int. J. Mach. Tools Manuf. **72**, 16–24 (2013)
17. I. Mancisidor, A. Urkiola, R. Barcena, J. Munoa, Z. Dombovan, M. Zatarain, Receptance coupling for tool point dynamic prediction by fixed boundaries approach. Int. J. Mach Tools Manuf. **78**, 18–29 (2014)
18. M. Leonesioa, P. Parentib, G. Bianchia, Frequency domain identification of grinding stiffness and damping. Mech. Syst. Signal Process. **93**, 545–558 (2017)
19. V. Tanuja, A. Chatterjee, Wavelet analysis of acceleration response of beam under the moving mass for damage assessment. J. Inst. Eng. (India): Ser. C. **97**, 209–221 (2016)
20. G. Chakraborty, On response of a single-degree-of-freedom oscillator with constant hysteretic damping under arbitrary excitation. J. Inst. Eng. (India): Ser. C. **97**, 579–582 (2016)
21. F. Montevecchi, N. Grossi, A. Scippa, G. Campatelli, Improved RCSA technique for efficient tool-tip dynamics prediction. Precis. Eng. **44**, 152–162 (2016)